Bulgarian Chemical Communications, Volume 51, Issue 4 (pp. 625 - 631) 2019 DOI: 10.34049/bcc.51.4.5056

Modeling the separation performance of nanofiltration and reverse osmosis: case study of groundwater desalination (M'Nasra zone Morocco)

M. Bchiti[1], M. Igouzal[2 *], F. El Azhar[1], H. Oudda[1], A. El Midaoui[1]

[1] *Laboratory of Separation Processes, Department of Chemistry, Faculty of Science, Ibn Tofail University, BP1246 Kenitra, Morocco*

[1] *Interdisciplinary Laboratory for Natural Resources and Environment, Department of Physics, Faculty of Science, Ibn Tofail University, BP1246 Kenitra, Morocco*

Received January21, 2019; Revised, May 7, 2019

Moroccan surface water and groundwater is enduring an increase of salt concentrations which exceed the drinking water standards. To solve this problem, in this study we will use membranes which are a helpful technique to reduce these concentrations and to achieve high water quality within the distribution system. This study is aimed at proposing a model of reverse osmosis experiments conducted in a pilot scale using synthetic water doped with NaCl. Firstly, performances were compared for different types of reverse osmosis membranes. Secondly, a mathematical model was applied on the experimental data. As a detailed characterization of the membranes utilized was not available, a simplified approach for the phenomenon as described in Spiegler-Kedem model was used. This model is based on irreversible thermodynamics and predicts the rejection performance of the system by an estimation of two coefficients: reflexion coefficient and permea bility coefficient. The Levenberg-Marquardt´s algorithm (LMA) was used which iteratively solves non-linear least-squares problems. Simulations are in good agreement with experimental data and the linear correlation coefficient for the fitted data was greater than 0.85 in all experiments. Application of the model showed that to enhance model predictions, experiments must be conducted in a wider range of pressures, especially those corresponding to lower energy need.

Keywords: Membrane processes, Osmosis, Permeate flux, Reverse salt rejection, Spiegler-Kedem model

INTRODUCTION

In most countries, water resources are scarce and under threat of industrial and urban wastes [1-4]. Wastewater treatment processes are used to treat municipal and industrial wastewater to meet effluent standards before discharging in the natural environment [5-8]. Morocco, like other southern Mediterranean countries, is enduring water shortage and a wide variation in levels of rainfall which is expected to aggravate over the next few years. Population concentrations followed by the industrial and agricultural activities along the coastal zone have led to an increase of drinking water demand along this area. To solve this problem, seawater and groundwater desalination is seen as a useful process. Hence, many desalination plants were built working through reverse osmosis (RO) process. On the other hand, nanofiltration (NF) is widely studied at laboratory and pilot scales. However, its implementation on an industrial scale is not yet well exploited. This technique was only implemented with removing nitrate from the groundwater of Sidi Taibi commune (near Kénitra Town) [9]. Desalination projects are expensive and high energy consuming, so that ready-to-use plants are not always available. Thus, it is decisive to choose the most appropriate membranes for a given water treatment project [10,11]. First, membrane performances must be studied in a pilot scale, especially where process uncertainties are potentially high, in terms of membranes performance and total operation cost [12,13].

In this study, we are interested in the desalination of M'Nasra's groundwater. This zone has been a subject to many studies. Bouya *et al.* [14] reported that during the last decade, M'Nasra aquifer has been subjected to an anarchic and non-rational groundwater abstraction, leading to an overexploitation of the aquifer, rupture of the hydrodynamic equilibrium, degradation of water quality. They have developed a hydrodynamic model to understand the spatial distribution of permeability and recharge, and have confirmed the nature of M'Nasra aquifer system hydrogeological functioning. Benseddik and Bouabid [15] studied the vulnerability of M'Nasra aquifer water based on three methods used to identify the most vulnerable areas that need a good management. Marouane *et al*. [16] studied the spatio-temporal variability of groundwater nitrate (NO^-) and pesticide in M'Nasra aquifer during 2012 and found that nitrate concentrations were higher than the critical value of 50 mg L^{-1}. Zouhri [17] reported that marine intrusion and the lithological composition of the

* To whom all correspondence should be sent:
E mail: mohammed.igouzal@uit.ac.ma

saline pre-Rifean nappes, combined with their tectonic structures and their flow towards the Rharb basin (including M'nasra zone), are considered as increasing factors behind the salinity of this area's underground water resources. For drinking water, the maximum acceptable concentration which WHO recommends is 250 mg L^{-1} for chloride and 200 mg L^{-1} for sodium [17].

This research is aimed at studying separation experiments by nanofiltration (NF) and reverse osmosis (RO) in a pilot scale laboratory. Measurements were conducted on synthetic groundwater from de M'Nasra zone (Morocco). Different membranes were used and their performances and selectivity towards sodium chloride salt (NaCl) were experimentally compared.

On the other hand, numerous phenomenological and mechanistic models have been proposed to describe solute and solvent transport through porous and dense membranes [18]. These mathematical models are based on conservation principles and include many parameters. Model parameter estimation is achieved by matching model predictions with experimental data. The development of these modeling techniques will successfully lead to a smaller number of experiments and subsequently save time and money in the developmental stage of a given project. For dense membranes, the solution-diffusion model is the most popular. In this model, solutes dissolve at the membrane interface and then diffuse through the membrane along the concentration gradient [19]. Pore-flow models also exist, in which different solutes are separated by size, frictional resistance, and/or charge. Finally, the Kedem-Katchalsky and Spiegler-Kedem (S-K) models employ irreversible thermodynamic arguments to derive solute and solvent transport equations while treating the membrane as a "black box" [20]. Models based on irreversible thermodynamics approach are the easiest to use, especially Spiegler-Kedem model which requires only two parameters for its application. This model is recommended for studies representing first attempts of modeling membranes processes. In addition, it is methodologically true to start with the simplest description of the phenomena under study, and to evaluate the limits of this approximation before investigating more complications. For all these reasons, the use of S-K model is adequate in our case study. Thereafter the capability of Spiegler-Kedem model to predict rejection performance was investigated [9,10].

M'Nasra aquifer belongs to the coastal area of Gharb basin. Geographically, it covers an area of approximately 600 km^2, and extends to 70 km along the coastal strip of Kenitra from the south and Moulay Bouselham from the north. It is bordered by Sebou River in the east, and the Atlantic Ocean in the west. This aquifer is the only resource of drinking water which supplies the population of many rural municipalities (Fig. 1) and irrigates various agricultural areas in the region.

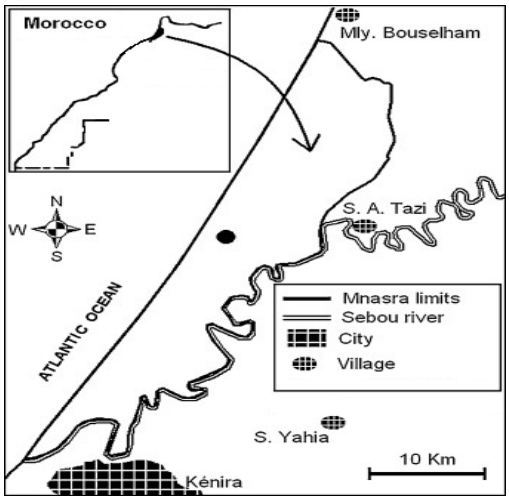

Fig. 1. Situation of the studied area

MATERIALS AND METHODS

Mathematical model

The performances of membranes were measured in terms of salts rejection (R) and permeate flux (Jv). For dilute aqueous mixtures consisting of water and a solute, the selectivity of a membrane toward the mixture is usually expressed in terms of the observed solute rejection coefficient. This parameter is a measure of a membrane's ability to separate the solute from the feed solution, and is defined, as a percentage:

$$R = 100\frac{C_f - C_p}{C_f}100\left(1\frac{C_p}{C_f}\right) \quad (1)$$

where C_p and C_f are the solute concentrations in the permeate and feed solution, respectively.

The Spiegler-Kedem (S-K) model, based on irreversible thermodynamics, provides a simple framework for description of solute transport in both RO and NF processes. In this model, the membrane is regarded as a "black-box" that can be characterized in terms of two coefficients: the solute permeability (Ps) and the reflection coefficient (σ). The S-K model considers convective coupling between solute and solvent species. This model has been successfully used to model solute retention in various applications, such as desalination of saline and brackish water, demineralization, etc. For the derivation of the S-K model, the starting point is the assumption that the water flux (Jw) and the solute flux (Js) are driven

by the forces F_w and F_s, respectively. These generalized forces are due to chemical potential gradients across the membrane:

$$J_w = L_{11}F_w + L_{12}F_s \text{ and } J_s = L_{21}F_w + L_{22}F_s \quad (2)$$

where L_{ij} are phenomenological coefficients.

The chemical potential gradient is caused by a concentration or pressure gradient. So that the final working equations of the nonlinear S-K model are:

$$J_w = L_P.\left(\frac{dP}{dx} - \sigma\frac{d\Pi}{dx}\right)$$

$$\text{and } J_s = P_s.\frac{dC_s}{dx} \ (1\sigma).C_s.J_w \quad (3)$$

where: J_w ($Kg.m^{-2}s^{-1}$): water flux; J_s ($Kg.m^{-2}s^{-1}$): solute flux; L_p ($m.s^{-1}$): solvent permeability constant; P (bar): operating pressure; Π (bar): osmotic pressure; x (m): distance across the membrane; Cs: solute concentration inside the membrane; Ps ($m.s^{-1}$): solute permeability constant; σ: reflection coefficient.

Solvent transport is due to the pressure gradient across the membrane and solute transport is due to the concentration gradient and convective coupling of the volume flow. Solute transport in RO membranes occurs predominantly *via* diffusion, however, for membranes with larger pores such as NF ones, both convective and diffusive contributions to the solute flux, are important and cannot be ignored [21].

Integration of equation (3) combined with relation (1) and considering the limit conditions of the problem (for x=0, $C_s=C_f$ and for x= Δx, $C_s=C_p$) lead to relation (4):

$$R = 1 - \frac{C_p}{C_f} = \frac{\sigma(1-F)}{1-\sigma F} \quad \text{with } F = \exp\left(-\frac{(1-\sigma)J_v}{P_s}\right) \quad (4)$$

where: C_f ($kg\,m^{-1}$): solute concentration in the feed solution; C_p ($kg\ m^{-3}$): solute concentration in the permeate solution; F (dimensionless): a flow parameter; Δx (m): membrane thickness.

The two transport parameters (σ and Ps) are the main parameters of the model. They are obtained by fitting the experimentally obtained rejection permeation data to the model calculated rejection. The parameter σ is a measure of the degree of membrane semi permeability, i.e. its ability to pass solvent in preference to solute. It characterizes the imperfection of the membrane [21]. The fitted coefficients are then said to represent the values of the transport coefficients for the given feed salt composition. Concentration dependence of these coefficients is assessed by fitting the data for different feed concentrations.

Pilot used

The experiments were performed on an NF/RO pilot plant (E 3039) supplied by TIA Company (Technologies Industrielles Appliquées, France). The pressure applied over the membrane can be varied from 5 to 70 bars by manual valves.

The pilot is equipped with two identical spiral wound modules operating in series. Each module contains one element. The pressure loss is about 2 bars corresponding to 1 bar of each module. Table 1 gives the characteristics of the commercial membranes used.

The experiments were performed at 20°C. Samples of permeate were collected and the water parameters were determined analytically following the standard methods.

Table 1. Characteristics of the membranes

Membrane	Surface (m^2)	P_{max}(bars)	Feed pH range	Max T(°C)	Material	Manifacturer
BW30LE4040	7.6	41	2-11	45	Polyamide	Filmtec
TMG10	8.0	40	2-11	45	Polyamide	Toray
TM710	8.0	41	3-9	45	Polyamide	Toray
NF90	7.6	40	3-10	45	Polyamide	Filmtec
NF270	7.6	40	3-10	45	Polyamide	Filmtec

Statistical analysis

In this study, a statistical analysis of residual errors was performed based on the Root Mean Square Error (RMSE), the Normalized Root Mean Square Error (NRMSE) and the Nash-Sutcliffe Efficiency (NSE) coefficient.

The RMSE is the distance, on average, of a data point from the fitted line. The NRMSE calculates the residual variance. The NSE is a normalized statistic that determines the relative magnitude of the residual variance (noise) compared to the measured data variance (information).

RESULTS AND DISCUSSION

RO on synthetic water doped with NaCl

Performances of RO membranes TMG10, TM710 and BW30LE4040 were first compared using synthetic water doped with NaCl at different dilutions as shown in table 2.

For a feed water salinity of 2 g L^{-1}, the influence of pressure on the permeate flux for the different membranes is shown in fig. 2 (a). An increase in applied pressure leads, as is to be expected from equation (4), to an increase in the permeate flux for all three tested membranes. Also, the permeate flux obtained with BW30LE4040 membrane is higher than that attained with other membranes. Fig. 2 (b) shows that the rejection coefficient of Cl^- is greater than 0.95 for the three membranes for all applied pressures. Rejection obtained with BW30LE4040 membranes is the lowest, in agreement with the high permeability of this membrane.

Table 2. Characteristics of the synthetic water doped with NaCl.

Salinity (g/l)	pH	Cl^-(ppm)	Na^+(ppm)
2	6.19	789.87	1203.58
4	6.02	1464.37	2482.396
6	6.3	1908.12	3272.22
8	6.44	2440.62	4983.59
10	6.62	3017.5	5641.8

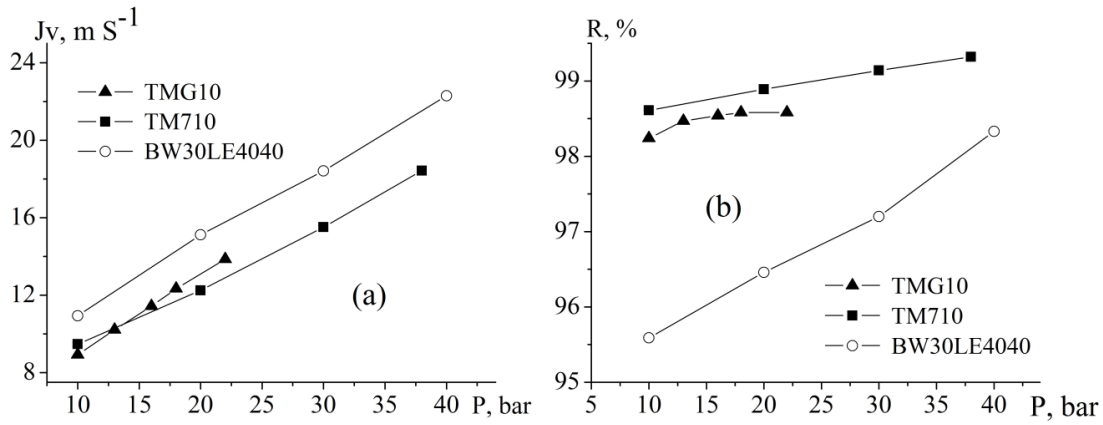

Fig. 2. (a) Variation of permeate flux and (b) rejection coefficient *(*for Cl^-) with pressure (for salinity of 2 g L^{-1}*)*

Fig. 3 shows the permeate flux as a function of pressure at different salinity concentrations (2, 6 and 10 g L^{-1}) for (a) TMG10, (b) TM710 and (c) BW30LE4040, respectively. As salinity concentration increases, permeate flux decreases for all three membranes used. Increasing feed concentration leads to an increase in osmotic pressure and hence permeate flux reduces (see equations 4 and 5).

On the other hand, high rejections are obtained with the three reverse osmosis membranes (greater than 95%) in concordance with manufacturer's specifications.

For all previous experiments, optimal values of coefficients σ and P were mathematically obtained by minimizing the model's cost function which is defined as the sum of the squared differences between predicted and observed values of the rejection coefficient.

Figure 4 shows a plot of the rejection coefficient (Cl^-, salinity concentration of 10 mg L^{-1}) as a function of the permeate flux for (a) TMG10, (b) TM710 and (c) BW30LE4040. As can be seen, calculations by the S-K model correctly reproduce the experimental data. The correlation coefficients calculated for the membranes TMG10, TM710 and BW30L4040 were equal to 0.93, 0.85 and 0.85, respectively. Table 3 summarizes the values of the parameters σ and Ps for all membranes at different salt concentrations. Increasing feed concentration leads to a decrease of reflection coefficient σ and an increase of permeate coefficient Ps in major cases.

Table 4 shows the results of the statistical analysis as described in material and methods section. The RMES coefficient obtained has a small value, the NRMSE function is smaller than unity and the NSE coefficient is very near to 1. This result demonstrates the good performance of the model and the optimization procedure.

Table 3. σ and Ps estimated by the model (Cl^-, salinity concentrations of 10 mg L^{-1})

Membrane	TM710			TMG10			BW30LE4040		
Salinity (mg/l)	2	6	10	2	6	10	2	6	10
σ	0.979	0.991	0.991	0.955	0.985	0.988	0.991	0.991	0.979
Ps (m/s)	1.10^{-7}	1.10^{-7}	2.10^{-7}	1.10^{-7}	2.10^{-7}	3.10^{-7}	2.10^{-7}	1.510^{-7}	$2.5.10^{-7}$

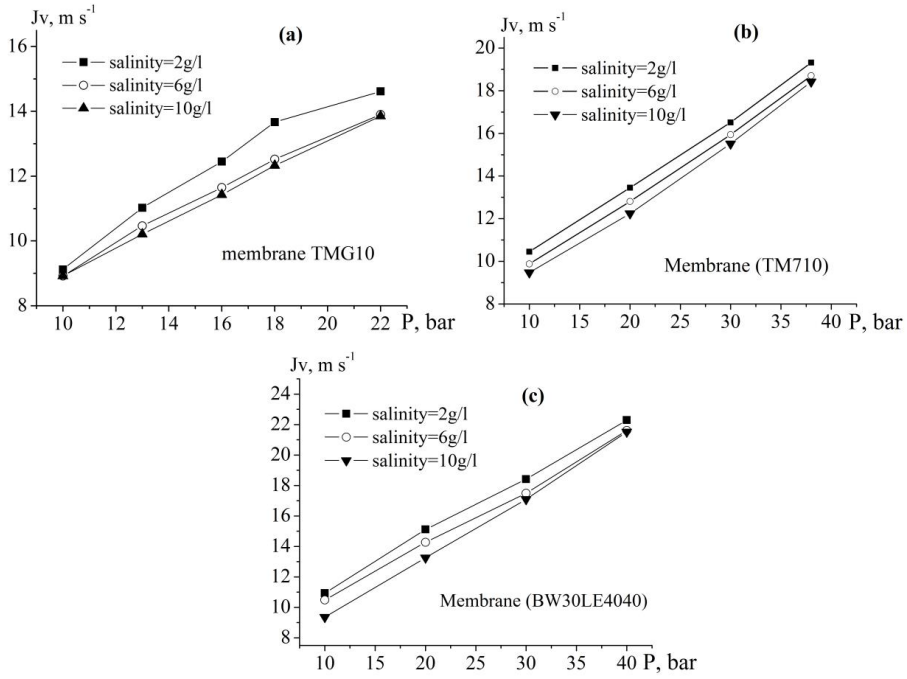

Fig 3. Variation of permeate flux with pressure for three salinity concentations: (a) TMG10 membrane, (b) TM710 membrane, (c) BW30LE4040 membrane

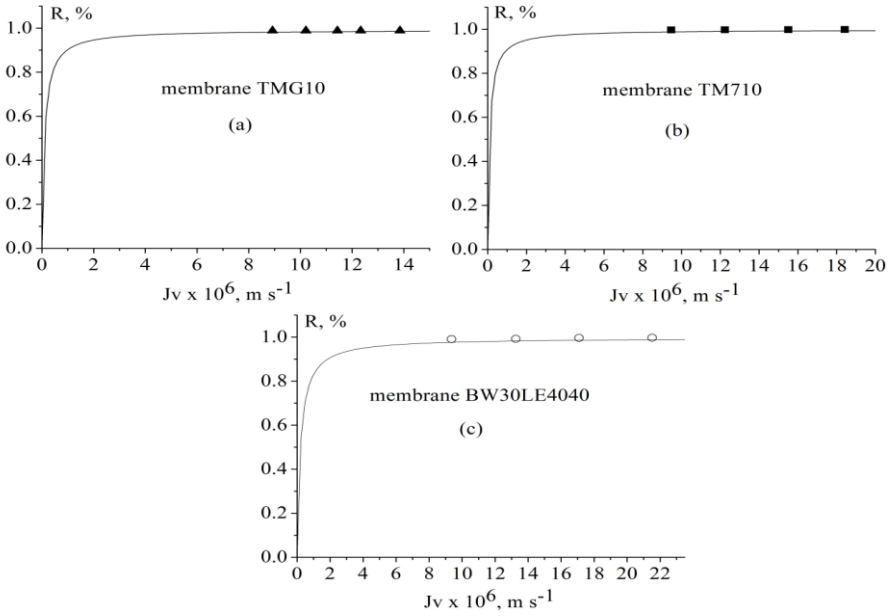

Fig. 4. Comparison between observed and predicted rejection (of Cl^-) for (a) TMG10, (b) TM710 and (c) BW30LE4040 (feed water salinity of 10 g L^{-1})

Table 4. Results of the statistical analysis

Membrane	RMSE (%)	NRMSE(-)	NSE (-)
TMG10	0.026	0.030	0.96
TM710	0.030	0.040	0.98
BW30LE40	0.029	0.060	0.99

Ground water treatment by RO and NF

In the second part of this research, ground water from M'Nasra zone was treated by reverse osmosis using BW30L4040 membrane, and by nanofiltration using NF90 and NF270 membranes. The characteristics of brackish water are shown in Table 5. Figure 5(a) shows the permeate flux as a function of pressure. For all membranes permeate flux increases linearly as pressure increases. The permeate flux obtained with NF membranes is higher than that with the BW30L4040 membrane. NF membranes are more permeable than RO membranes because of the presence of nanoporosity in NF while the RO membrane is dense. Figure 5(b) presents the retention coefficient of Cl^- as a function of the applied pressure. The Cl^- retention with BW30L4040 membrane is the highest and pressure independent. For NF membranes, there is an increase in retention with increased applied pressure. Also, retention is more important for NF90 membrane than for NF270 membrane.

Application of S-K model leads to reflection coefficients (σ) and solute permeability coefficients (Ps) shown in Table 6.

Table 5. Characteristics of the feed water

Parameters	Brackish water	Moroccan standards	Standards World Health Organization
T °C	23	-	25
pH	8.08	6.0 - 9.2	6.5-8.5
TDS (ppm)	2690	< 1000	< 1000
Na^+ (ppm)	780.12	100	< 200
Cl^- (ppm)	1325	350 - 750	< 250
Mg^{2+} (ppm)	87.50	100	< 50
Ca^{2+} (ppm)	20	< 500	< 270
SO_4^{2-} (ppm)	125.88	200	< 200

Figure 6 shows a plot of the rejection coefficient as a function of the permeate flux. Calculated and experimental rejection coefficients are very close. Correlation coefficients for BW30L4040, NF90 and NF270 were equal to 0.91, 0.85, and 0.85, respectively.

Also, as for synthetic water, statistical indicators (RMES, NRMSE and NSE) for ground water were very satisfactory.

Table 6. Model constants σ and Ps estimated by the model

Membrane	NF90	NF270	BW30L4040
σ	0.925	0.576	0.988
Ps (m/s)	0.14	0.7	0.04

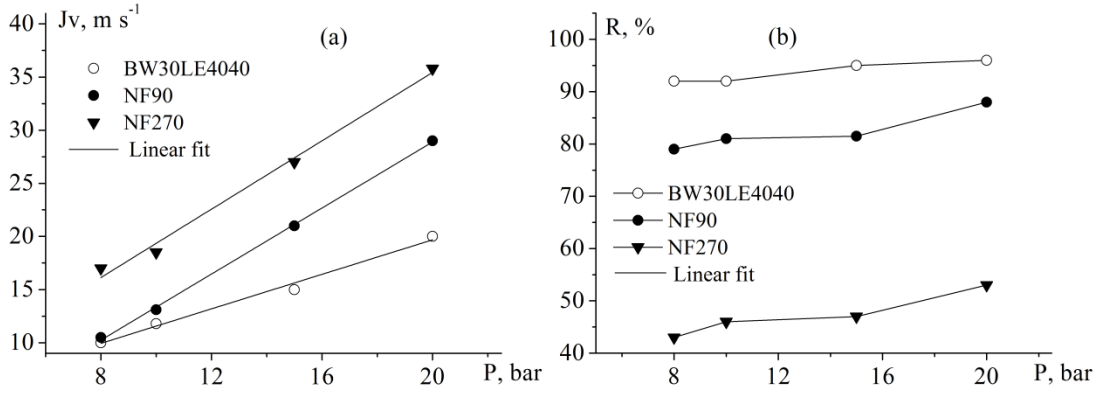

Fig. 5. (a) Variation of permeate flux and (b) rejection coeficient (for Cl^-) with pressure

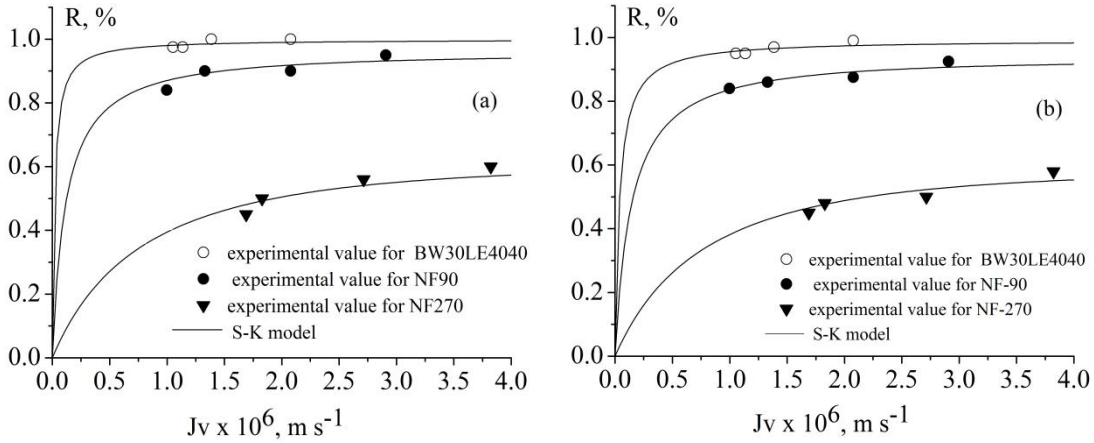

Fig. 6. Comparison between observed and predicted Cl^- and Na^+

CONCLUSION

The aim of this research was to study separation experiments by nanofiltration (NF) and reverse osmoses (RO) in a laboratory pilot scale. Experiments were conducted on synthetic water doped with NaCl and on groundwater from the M'Nasra zone (Morocco). Different sizes of membranes were used (RO and NF membranes) and their performances and selectivities towards sodium chloride salt (NaCl) were experimentally compared.

A first attempt was undertaken to model the separation tests using Spiegler-Kedem model. The simulation results were found to be in good agreement with the experimental data since the coefficient of determination obtained for the fitted data was greater than 0.85 in all experiments. Model results were used to verify the consistency of the experimental measurements in order to improve the procedure. The study has shown that to enhance the output of the model, pilot experiments must be conducted in a wider range of pressures, especially at pressures from 5 to 8 bar which correspond to lower energy consumption. Simulations (models coefficient) remain valid in the range of the concentration and experimental conditions used. Other measurements (made under different conditions) can be used to test the robustness of the model. Also, results of this study are obtained with no information on membranes characteristics. A detailed knowledge of these characteristics can improve the predictability of their filtration performance. Our future development may focus on amelioration of the modeling approach by a better description of the membranes and the transport mechanism occurring inside them.

REFERENCES

1. A. Shokri, *Bulg. Chem. Commun.*, **50**, 27 (2018).
2. A. Shokri, *Int. J. Nano Dimens.*, **7**, 160 (2016).
3. A. Shokri, *Russ. J. Appl. Chem.*, **88**, 2038 (2015).
4. M. Mohadesia, A. Shokri, *Desal. Water Treat.*, **81**, 199 (2017).
5. A. Shokri, A. Hassani, *Russ. J. Appl. Chem*, **89**, 1985 (2016).
6. A. Shokri, K. Mahanpoor, *Int. J. Ind. Chem*.**8**, 101, (2017).
7. A. Shokri, *Desal. Water Treat.*, **111**, 173 (2018)
8. A. Shokri, *Desal. Water Treat.*, **58,** 258 (2017).
9. M. Igouzal, F. El Azhar, M. Hafsi, M. Taky, A. Elmidaoui, *Desal. Water Treat.*, **93**, 30 (2017).
10. S. Zarinabadi, *Bulg. Chem. Commun.*, **48**, 112 (2016).
11. A. Shokri, M. Nasiri Shoja, *Bulg. Chem. Commun*, **50**, 1 (2018).
12. N. Zouhri, M. Igouzal, M. Larif, M. Hafsi, M. Taky, A. Elmidaoui, *Desal. Water Treat*, accepted, doi:10.5004/dwt.2018.21410.
13. A. S. M. Tabatabaee Ghomshe, *Bulg. Chem. Commun.*, **48**, 57 (2016).
14. B. Bouya, M. Faouzi, M. Ben Abbou, A. Essahlaoui, M. Bahir, N. Youbi, M A. Hessane, *Comunicações Geológicas,* **98**, 73 (2011).
15. B. Benseddik, E.M. Bouabid, *Arab. J. Earth Sci.*, **3**, 14 (2016).
16. B. Marouane, K. Belhsain, M. Jahdi, S. K. Belhsain, M. Jahdi, S. El Hajjaji, A. Dahchour, S. Dousset, A. Satrallah, *J. Mater. Environ. Sci*., **5**, 2151 (2014).
17. L. Zouhri, *J. Envir. Hydrol.*, **11**, 1 (2003).
18. J. Wang, D.S. Dlamini, A.K., Mishra, *J. Membrane Sci.*, **454**, 516 (2014).
19. M.F. San Román, E. Bringas, R. Ibañez, I. J. Ortiz, *J. Chem. Technol. Biotechnol.*, **85**, 2 (2010).
20. V. Nikonenko, V. Zabolotsky, C. Larchet, B. Auclair, G. Pourcelly, *Desalination*, 147, **369** (2002).
21. O. Kedem, K.S. Spiegler, *Desalination*, **1**, 311 (1966).